

# **SAND REPORT**

SAND2002-4135

Unlimited Release

Printed December 2002

## **FY02 Field Evaluations of an In-Situ Chemiresistor Sensor at Edwards Air Force Base, CA**

Clifford K. Ho, Lucas K. McGrath, and James May

Prepared by  
Sandia National Laboratories  
Albuquerque, New Mexico 87185 and Livermore, California 94550

Sandia is a multiprogram laboratory operated by Sandia Corporation,  
a Lockheed Martin Company, for the United States Department of  
Energy under Contract DE-AC04-94AL85000.

Approved for public release; further dissemination unlimited.



Issued by Sandia National Laboratories, operated for the United States Department of Energy by Sandia Corporation.

**NOTICE:** This report was prepared as an account of work sponsored by an agency of the United States Government. Neither the United States Government, nor any agency thereof, nor any of their employees, nor any of their contractors, subcontractors, or their employees, make any warranty, express or implied, or assume any legal liability or responsibility for the accuracy, completeness, or usefulness of any information, apparatus, product, or process disclosed, or represent that its use would not infringe privately owned rights. Reference herein to any specific commercial product, process, or service by trade name, trademark, manufacturer, or otherwise, does not necessarily constitute or imply its endorsement, recommendation, or favoring by the United States Government, any agency thereof, or any of their contractors or subcontractors. The views and opinions expressed herein do not necessarily state or reflect those of the United States Government, any agency thereof, or any of their contractors.

Printed in the United States of America. This report has been reproduced directly from the best available copy.

Available to DOE and DOE contractors from

U.S. Department of Energy  
Office of Scientific and Technical Information  
P.O. Box 62  
Oak Ridge, TN 37831

Telephone: (865)576-8401  
Facsimile: (865)576-5728  
E-Mail: [reports@adonis.osti.gov](mailto:reports@adonis.osti.gov)  
Online ordering: <http://www.doe.gov/bridge>

Available to the public from

U.S. Department of Commerce  
National Technical Information Service  
5285 Port Royal Rd  
Springfield, VA 22161

Telephone: (800)553-6847  
Facsimile: (703)605-6900  
E-Mail: [orders@ntis.fedworld.gov](mailto:orders@ntis.fedworld.gov)  
Online order: <http://www.ntis.gov/help/ordermethods.asp?loc=7-4-0#online>



SAND2002-4135  
Unlimited Release  
Printed December 2002

## **FY02 Field Evaluations of an In-Situ Chemiresistor Sensor at Edwards Air Force Base, CA**

Clifford K. Ho and Lucas K. McGrath  
Sandia National Laboratories  
P.O. Box 5800  
Albuquerque, New Mexico 87185-0735  
Contact: ckho@sandia.gov  
(505) 844-2384

James May  
Earth Tech  
100 West Broadway, Suite 240  
Long Beach, CA 90802-4443

### **Abstract**

The design, operation, and performance of an in-situ chemiresistor sensor were evaluated during field tests at Edwards Air Force Base in FY02. The primary objectives of the tests were to evaluate the ruggedness of the waterproof sensor housing and to test the operation and performance of the chemiresistor sensor in both the unsaturated and saturated zones of a contaminated well (18-MW37). The housing was tested by lowering it to greater and greater depths beneath the water table over the course of two months. Results showed that the polymer membrane that allows volatile organic compound (VOC) vapors to partition to the sensors inside the housing was able to withstand approximately 30 ft (9 m) of water pressure before allowing liquid to penetrate into the housing. Corrosion of the 304 stainless-steel housing was observed, but the integrity of the housing was not compromised during the tests. With regard to the operation and performance of the chemiresistor sensor, tests showed that the chemiresistor was able to operate continuously over a four-month testing period in contaminated and corrosive aqueous environments. Data were logged continuously using a Campbell Scientific CR10X data logger powered by a 12 amp-hour battery connected to a 20-watt solar panel. Samples taken from the well during the tests (and analyzed in the laboratory) revealed that the concentrations of contaminants (e.g., TCE) in the vicinity of the chemiresistor were lower than the detection limits of the chemiresistor, so direct comparisons could not be made. Results did indicate, however, that the high-humidity environments (100%) caused instability in the chemiresistor readings that produced anomalously high estimates of VOC concentrations. Improvements to both the stability and sensitivity of the chemiresistor sensors are currently being investigated through the use of automated temperature control and an integrated preconcentrator assembly.

## **Acknowledgments**

The authors thank Mary Spencer, Irene Nester, and Tara MacHarg for their project-management support and Chad Davis for his calibration of the chemiresistor sensor. This work was funded by Edwards AFB through a Work for Others contract #061010824-0 (MIPR #W62N6M12477926). Sandia is a multiprogram laboratory operated by Sandia Corporation, a Lockheed Martin Company, for the United States Department of Energy under Contract DE-AC04-94AL85000.

# Contents

<b>1. Introduction</b>	<b>9</b>
1.1 Overview and Objectives	9
1.2 Chemiresistor Sensor and Package	9
1.3 Chemiresistor Calibration and Sensitivity	11
1.4 Background on Edwards Air Force Base and the Field-Test Site	12
<b>2. Phase I: Field Evaluation of Sensor Package</b>	<b>14</b>
2.1 Approach	14
2.2 Results	16
2.2.1 Water-Entry-Pressure Threshold	16
2.2.2 Corrosion	17
<b>3. Phases II and III: Field Evaluation of Chemiresistor Performance in the Unsaturated and Saturated Zones</b>	<b>18</b>
3.1 Approach	18
3.2 Temperature, Pressure, and Relative Humidity	21
3.3 Analytical Results from Laboratory Samples	22
3.4 Chemiresistor Results	23
3.4.1 Initial Week-Long Test	23
3.4.2 Unsaturated-Zone Test	24
3.4.3 Saturated-Zone Test	25
3.4.4 Transient Test	27
3.4.5 Results of Long-Term Evaluation	28
<b>4. Discussion of Results and Objectives</b>	<b>29</b>
4.1 Objectives of Edwards Air Force Base In-Situ Sensor Program	29
4.2 Objective 1: Longevity of Sensor Housing	30
4.3 Objectives 2, 3, 4, and 5: Chemiresistor Performance	30
4.4 Objective 6: Operation and Maintenance Requirements	31
4.5 Objectives 7 and 8: Potential Use at Edwards Air Force Base	31
<b>5. Summary and Recommendations</b>	<b>32</b>
<b>6. References</b>	<b>33</b>
<b>7. Appendices</b>	<b>34</b>
7.1 Appendix A: Campbell Scientific CR10X Data-Logging Program	34
7.2 Appendix B: Calibration Curves for Chemiresistor Sensor	37

## List of Figures

Figure 1. VOC detection by a thin-film chemiresistor: (a) Electrical current (I) flows across a conductive thin-film carbon-loaded polymer deposited on a micro-fabricated electrode; (b) VOCs absorb into the polymer, causing it to swell (reversibly) and break some of the conductive pathways, which increases the electrical resistance. ....	10
Figure 2. Chemiresistor array (chip C12) developed at Sandia National Laboratories with four conductive polymer films deposited onto a microfabricated circuit. A temperature sensor (middle) and heating elements (ends) are also integrated. ....	10
Figure 3. Stainless-steel waterproof package that houses the chemiresistor array. Left: GORE-TEX <sup>®</sup> membrane covers a small window over the chemiresistors. Right: Disassembled package exposing the 16-pin dual-in-line package and chemiresistor chip. ....	11
Figure 4. Map of Edwards Air Force Base and surrounding areas. ....	13
Figure 5. Lowering the chemiresistor sensor housing down well 18-MW37 for the Phase I test (11/14/2001). ....	14
Figure 6. Chemiresistor sensor package with the cap removed, exposing the 16-pin sensor package. A red “X” was drawn on a tissue to indicate if water was leaking into the housing. ....	15
Figure 7. Weekly visual inspection of the housing interior (no chemiresistor chip). Left: Smearred red “X” after the housing had been submerged for 6 weeks (depth below water table was increased to 32 feet). Right: Liquid water observed in the housing after 9 weeks. ....	15
Figure 8. Evidence of corrosion and microbial activity. Left: Black spots were observed on the threads of the housing after 2 weeks of immersion. Middle: “Slime” observed at 9 weeks (began at 2 weeks). Right: Corrosion was observed near the seam and O-ring of the housing at 10 weeks (began at 5 weeks). ....	18
Figure 9. Left: Three sensors were deployed in Phases II and III (temperature/humidity probe, chemiresistor probe, and pressure transducer). Right: Tethering the sensors together before lowering them down well 18-MW37. ....	19
Figure 10. Left: Assembling the data-logging station at well 18-MW37. Right: Anchoring the tripod to the ground. ....	19

Figure 11. Left: Lowering sensors down well 18-MW37. Middle: View of cables from top of well casing. Right: Downloading data from the data logger. ....	20
Figure 12. Barometric pressure in well 18-MW37. ....	22
Figure 13. Response of the chemiresistor sensors during the first week. The chemiresistor probe was immersed by the rising water table. Baseline resistance was taken from dry conditions in the Earth Tech trailer (23°C, ~24% RH). ....	24
Figure 14. Relative percent change of the chemiresistor resistances during the Phase II unsaturated-zone test (June 6 – June 25, 2002). The baseline resistances were taken at the beginning of the test on June 6, 2002. ....	25
Figure 15. Estimated TCE vapor concentrations during the Phase II unsaturated-zone test. ....	25
Figure 16. Relative percent change of the chemiresistor resistances during the Phase III unsaturated-zone test (June 27 – September 5, 2002). The baseline resistances were taken at the beginning of the test on June 27, 2002. ....	26
Figure 17. Estimated aqueous TCE concentrations during the Phase III saturated-zone test. ....	27
Figure 18. Relative percent change of the chemiresistor resistances during the transient test on September 5, 2002. The baseline resistances were taken while the chemiresistor was suspended 37 ft below TOC. ....	28
Figure 19. Measured chemiresistor resistances during all field tests (May – September 2002). ....	29
Figure 20. Integrated preconcentrator/chemiresistor assembly in the waterproof package. ....	31
Figure 21. Calibration curves for PECH polymer on chip C12. ....	37
Figure 22. Calibration curves for PNVP polymer on chip C12. ....	38
Figure 23. Calibration curves for PIB polymer on chip C12. ....	38
Figure 24. Calibration curves for PEVA polymer on chip C12. ....	39

## List of Tables

Table 1. Results of housing-immersion test at 18-MW37. ....	16
Table 2. Notable events during Phases II and III of chemiresistor operational tests. ....	20
Table 3. Laboratory analysis of gas and liquid samples taken from 18-MW37. <sup>1</sup> .....	22

# 1. Introduction

## 1.1 Overview and Objectives

This report summarizes work performed in FY02 at Edwards Air Force Base to evaluate the performance of an in-situ chemiresistor sensor developed at Sandia National Laboratories. A “Work for Others” contract in the amount of \$25K was awarded to Sandia to deploy and evaluate the sensor at an Edwards Air Force Base site contaminated with volatile organic compounds (VOCs). The purpose of the tests was to evaluate the robustness, longevity, and capabilities of the sensor and packaging in a real field environment. The assessment was intended to help determine necessary areas for improvement in the development of the chemiresistor sensors. In addition, the objective for Edwards Air Force Base was to test and evaluate this sensor and other emerging technologies to identify cheaper and more effective methods for monitoring, characterizing, and remediating their contaminated sites. With these global objectives in mind (more detailed objectives are discussed in Section 4), three primary tasks were proposed for FY02:

- Phase I: Test the robustness of the chemiresistor sensor housing by lowering the housing beneath the water table at a contaminated well and checking for leaks and material degradation
- Phase II: Test the performance of the chemiresistor sensor in the vadose zone
- Phase III: Test the performance of the chemiresistor sensor in the saturated zone

The remainder of this section provides background material regarding the physics of the chemiresistor sensor and its packaging, along with an overview of the test site. Subsequent sections in this report describe the results of each of the three phases of testing at Edwards Air Force Base. Recommendations regarding areas of needed improvement and potential applications of the chemiresistor sensor are also presented.

## 1.2 Chemiresistor Sensor and Package

The chemiresistor sensor used in the tests at Edwards Air Force Base is essentially a chemically sensitive resistor comprised of a conductive polymer film on a micro-fabricated circuit. The chemically-sensitive polymer is dissolved in a solvent and mixed with conductive carbon particles. The resulting ink is then deposited and dried onto thin-film platinum traces on a solid substrate (chip). When chemical vapors come into contact with the polymers, the chemicals absorb into the polymers, causing them to swell. The swelling changes the resistance of the electrode, which can be measured and recorded using a data logger or an ohmmeter (see Figure 1). The swelling is reversible if the chemical vapors are removed, but some hysteresis can occur at high concentration exposures. The amount of swelling corresponds to the concentration of the chemical vapor in contact with the chemiresistor, so these devices can be calibrated by exposing the chemiresistors to known concentrations of target analytes.

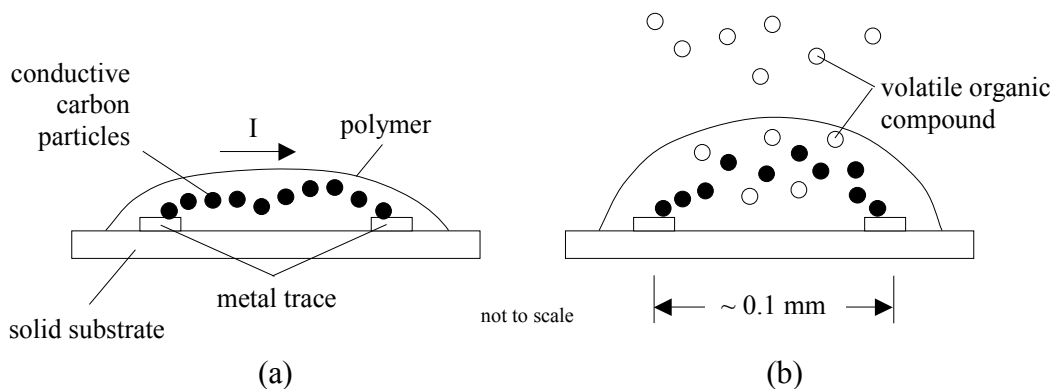


Figure 1. VOC detection by a thin-film chemiresistor: (a) Electrical current ( $I$ ) flows across a conductive thin-film carbon-loaded polymer deposited on a micro-fabricated electrode; (b) VOCs absorb into the polymer, causing it to swell (reversibly) and break some of the conductive pathways, which increases the electrical resistance.

Two unique features exist regarding the chemiresistor sensor package used in these tests. First, the architecture of the microsensors (Hughes et al., 2000) integrates an array of chemiresistors with a temperature sensor and heating elements (Figure 2). The chemiresistor array has been shown to detect a variety of VOCs including aromatic hydrocarbons (e.g., benzene), chlorinated solvents (e.g., trichloroethylene (TCE), carbon tetrachloride), aliphatic hydrocarbons (e.g., hexane, iso-octane), alcohols, and ketones (e.g., acetone). The on-board temperature sensor comprised of a thin-film platinum trace can be used to not only monitor the in-situ temperature, but it can also provide a means for temperature control. A feedback control system between the temperature sensor and on-board heating elements can allow the chemiresistors to be maintained at a fairly constant temperature, which can aid in the processing of data when comparing the responses to calibrated training sets. In addition, the chemiresistors can be maintained at a temperature above the ambient to prevent condensation of water, which may be detrimental to the wires and surfaces of the chemiresistor. However, a fieldable version of the automated temperature control has just recently been tested in the laboratory, and it was not implemented in the field tests at Edwards Air Force Base.

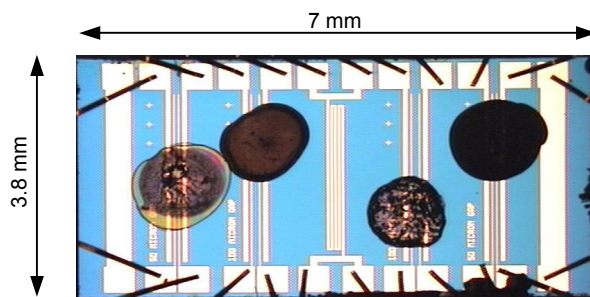


Figure 2. Chemiresistor array (chip C12) developed at Sandia National Laboratories with four conductive polymer films deposited onto a microfabricated circuit. A temperature sensor (middle) and heating elements (ends) are also integrated.

A second unique feature is that a robust package has been designed and fabricated to house the chemiresistor array (Ho and Hughes, 2002). This cylindrical package is small (~ 3 cm diameter) and is constructed of rugged, chemically-resistant material. Early designs have used PEEK (PolyEtherEtherKetone), a semi-crystalline, thermoplastic with excellent resistance to chemicals and fatigue. Newer package designs have been fabricated from stainless steel (Figure 3). The package design is modular and can be easily taken apart (unscrewed like a flashlight) to replace the chemiresistor sensor if desired. Fitted with Viton O-rings, the package is completely waterproof, but gas is allowed to diffuse through a GORE-TEX<sup>®</sup> membrane that covers a small window to the sensor. Like clothing made of GORE-TEX<sup>®</sup>, the membrane prevents liquid water from passing through it, but the membrane “breathes,” allowing vapors to diffuse through. Even in water, dissolved VOCs can partition across the membrane into the gas-phase headspace next to the chemiresistors to allow detection of aqueous-phase contaminants. The aqueous concentrations can be determined from the measured gas-phase concentrations using Henry’s Law. Mechanical protection is also provided via a perforated metal plate that covers the chemiresistors. The chemiresistors are situated on a 16-pin dual-in-line package that is connected to a weatherproof cable, which can be of any length because of the DC-resistance measurement. The cable can be connected to a hand-held multimeter for manual single-channel readings, or it can be connected to a multi-channel data logger for long-term, remote operation.

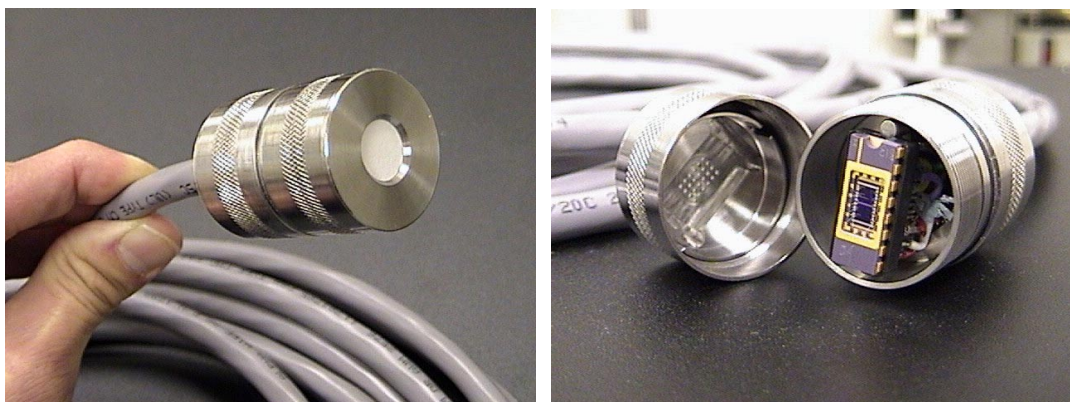


Figure 3. Stainless-steel waterproof package that houses the chemiresistor array. Left: GORE-TEX<sup>®</sup> membrane covers a small window over the chemiresistors. Right: Disassembled package exposing the 16-pin dual-in-line package and chemiresistor chip.

### 1.3 Chemiresistor Calibration and Sensitivity

The chemiresistors are calibrated by exposing the chemiresistor arrays to known concentrations of analytes of interest. The change in resistance corresponding to different VOC concentrations is recorded. These calibrations can be conducted under a variety of relative humidity and temperature conditions to provide a suite of training sets that can be used when the chemiresistor is exposed to varying conditions in the field.

The sensitivity of these devices depends on the type of polymer used in the chemiresistor, thickness of the polymer film, the amount of carbon particles added to polymer, separation distance between the electrodes, and the type of analyte. A general observation for the chemiresistors developed at Sandia is that the best chemiresistors for a particular vapor can detect vapor concentrations on the order of  $1/1000^{\text{th}}$  (or 0.1%) of the saturated vapor pressure of the analyte being detected. For some VOCs, this detection limit is below the maximum concentration limits set forth by the United States Environmental Protection Agency for air and drinking water (U.S. EPA). For example, m-xylene was reliably detected at  $1/100^{\text{th}}$  its saturated vapor pressure, or approximately 100 parts per million (ppm) by volume in the gas phase. According to Henry's Law, this corresponds to  $\sim 2$  ppm by mass in the aqueous phase, which is less than the 10 ppm maximum concentration limit imposed by the U.S. EPA. However, for TCE, the chemiresistors can detect gas-phase concentrations as low as 100-1000 ppm, which corresponds to an aqueous TCE concentration of  $\sim 1$ -10 ppm. The U.S. EPA maximum concentration limit for TCE in drinking water is 0.005 ppm, well below the current detection limits. Nevertheless, many applications such as pre-screening and remediation monitoring do not require the capability to provide such low detection limits. In addition, efforts are ongoing to develop integrated preconcentrators that can increase the apparent sensitivity of the chemiresistor sensors.

#### **1.4 Background on Edwards Air Force Base and the Field-Test Site**

Edwards Air Force Base is located in the Mojave Desert, north of Los Angeles, CA (see Figure 4). Edwards Air Force Base is located at an elevation of approximately 2,300 feet (700 m) above sea level, and the average rainfall is approximately 5 inches per year. Average temperatures in the summer range from a low of 65°F (18°C) to a high of 95°F (35°C), and average temperatures in the winter range from a low of 35°F (2°C) to a high of 60°F (16°C).

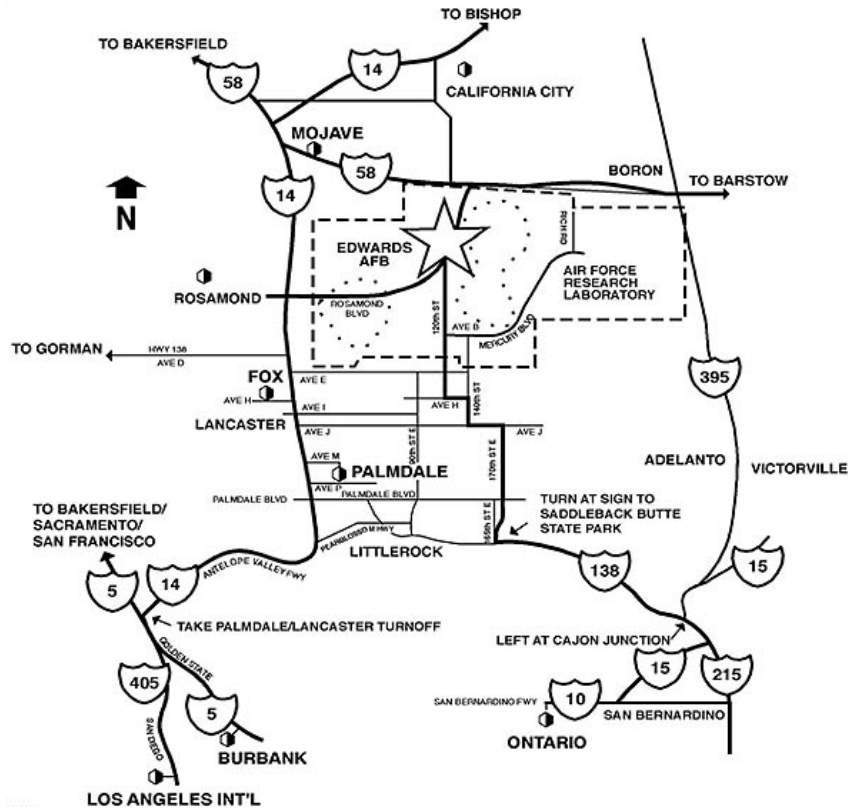


Figure 4. Map of Edwards Air Force Base and surrounding areas.

Edwards AFB serves as a flight-test research center, providing research, development, and testing of military and commercial aerospace systems for the United States. Several locations at Edwards AFB have been contaminated with petroleum products and chlorinated solvents that have seeped into the subsurface. For example, Site 18 (approximately 20 acres in size with four large aircraft hangars) has a large plume of chlorinated solvents encompassing a petroleum related contaminant. A primary contaminant found in the groundwater at this site is trichloroethylene (TCE), which had been measured as high as 56 ppm (well 18-T22 on 2/2/00). A dual extraction system began operation in April of 2000 to remediate both the groundwater and vapors at this site.

The field tests described in this report were conducted at Site 18 at monitoring well 18-MW37. The 4-inch-diameter well, constructed in 1998, is 101 ft deep and screened between 85 and 100 ft. The water level on April, 2001, was approximately 27 ft below the top of the well casing (TOC), but the operation of a dual-extraction system has lowered the water level.

Phase I (testing the chemiresistor housing) was performed between the months of November 2001 and January 2002. Phases II and III (testing the performance of the chemiresistor sensor in the unsaturated and saturated zones) were performed between May 2002 and October 2002.

## 2. Phase I: Field Evaluation of Sensor Package

### 2.1 Approach

As detailed in the previous section, the stainless-steel housing that encases the chemiresistor sensors is sealed with Viton O-rings, and a Gore-Tex<sup>®</sup> polymer membrane prevents liquid water from entering the window that is used to allow vapors to diffuse and partition to the sensors. However, the Gore-Tex<sup>®</sup> membrane has a water-entry-pressure threshold that, when exceeded, will allow liquid water to seep through the membrane. The membrane used in this test (PreVent<sup>®</sup> #VE61221) has a manufacturer-specified water-entry-pressure threshold of 20 psi (46 feet of water head), but this prescribed value is for temporary conditions and does not apply to long-term submersion conditions (personal communication, Steve DelRosso, product manager, W.L. Gore & Associates).

The purpose of this test was to determine the long-term water-entry-pressure threshold by lowering the housing to greater and greater depths beneath the water table at well 18-MW37 (Figure 5). A small piece of tissue was placed where the chemiresistor sensors would normally reside in the housing, and a small red “X” was marked on the tissue, which would smear if water leaked into the housing (see Figure 6). On November 14, 2001, the housing was placed two feet below the water table in well 18-MW37. A week later, the sensor package was pulled up, inspected, and then lowered an additional five feet below the water table. This process continued on a weekly basis until leakage occurred.



Figure 5. Lowering the chemiresistor sensor housing down well 18-MW37 for the Phase I test (11/14/2001).

In addition, the ability for the housing to withstand corrosion was also investigated. The water at well 18-MW37 was contaminated with low concentrations of volatile organic compounds, and

sulfur-based fuel additives also existed in the water that may yield conditions conducive to corrosion of metals. Previous equipment and materials placed in the water at this site showed significant signs of corrosion. Therefore, the condition of the housing was inspected weekly to determine if corrosion was occurring.



Figure 6. Chemiresistor sensor package with the cap removed, exposing the 16-pin sensor package. A red “X” was drawn on a tissue to indicate if water was leaking into the housing.

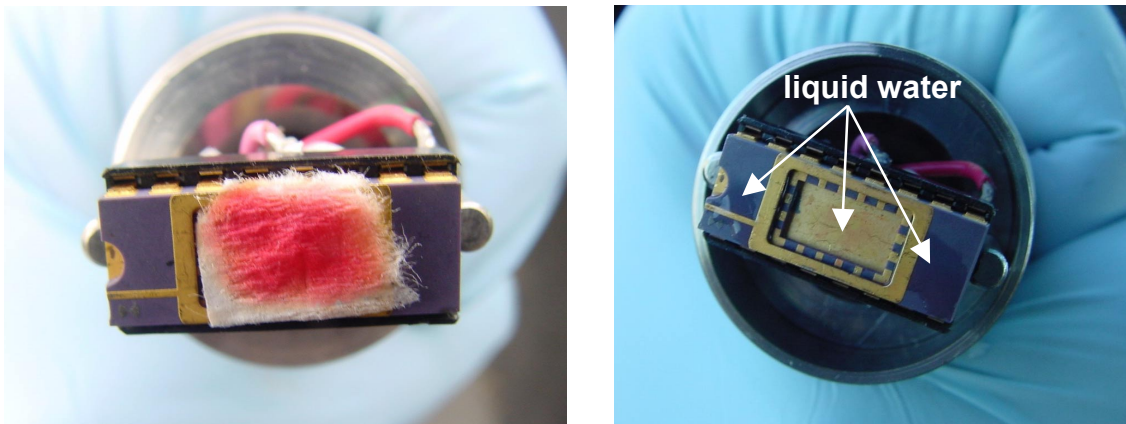


Figure 7. Weekly visual inspection of the housing interior (no chemiresistor chip). Left: Smears red “X” after the housing had been submerged for 6 weeks (depth below water table was increased to 32 feet). Right: Liquid water observed in the housing after 9 weeks.

## 2.2 Results

### 2.2.1 Water-Entry-Pressure Threshold

Results of the test (see Table 1) showed that the Gore-Tex<sup>®</sup> membrane withstood depths of up to ~30 feet below the water table (~13 psi) before allowing water to seep into the housing. After six weeks of continual immersion at increasing depths, we finally observed signs of moisture within the housing as evidenced by the smeared red “X” (see Figure 7). The sensor was placed at reduced depths beneath the water table (higher elevations) during subsequent weeks. The sensor was eventually raised to just five feet below the water table, but the housing continued to show signs of leakage (Figure 7). We suspect that the performance of the membrane may have been compromised once it was initially breached. However, later tests in Phase III showed that the membrane, which had been replaced, and housing were able to prevent water leakage for at least four months when the immersion depths were maintained at less than 5 feet beneath the water table.

It should be noted that the observed water-entry-pressure threshold of ~30 feet (~13 psi) is about 65% of the manufacturer-specified value of 20 psi. The difference is attributed to the continuous long-term immersion of the membrane in the current test, which contrasts the short-term tests conducted by the manufacturer. Alternative polymer laminates are available from W.L. Gore & Associates that have larger water-entry pressure ratings. Custom membranes are available that are rated at 250 psi, but assuming that that long-term continuous immersion will decrease this threshold by the same percentage as observed in the current test, the water-entry-pressure threshold of these new samples would be approximately 163 psi, or approximately 114 feet of water head. These samples have not yet been tested.

Table 1. Results of housing-immersion test at 18-MW37.

Date	Water Table Depth (feet below top of casing)	Sensor Depth Below Water Table (feet)	Results of Visual Inspection	Notes
11/14/01	33.8	2.00	<ul style="list-style-type: none"> <li>no corrosion; no staining</li> <li>no moisture; clear red X</li> </ul>	1,4
11/21/01	32.91	7.00	<ul style="list-style-type: none"> <li>no corrosion; no staining</li> <li>no moisture; clear red X</li> </ul>	2,3
11/29/01	33.19	12.00	<ul style="list-style-type: none"> <li>no corrosion; slight slime; black spots forming on inside threads</li> <li>no moisture; clear red X</li> </ul>	1,4
12/06/01	33.29	17.00	<ul style="list-style-type: none"> <li>no corrosion; slight slime; black spots on inside threads</li> <li>no moisture; clear red X</li> </ul>	1,4
12/12/01	33.47	22.00	<ul style="list-style-type: none"> <li>no corrosion; slime; black spots on inside threads</li> <li>no moisture; clear red X</li> </ul>	1,4
12/19/01	33.41	27.00	<ul style="list-style-type: none"> <li>corrosion near O-ring; slight slime; black spots on inside threads</li> <li>no moisture; clear red x</li> </ul>	1,4

Date	Water Table Depth (feet below top of casing)	Sensor Depth Below Water Table (feet)	Results of Visual Inspection	Notes
12/27/01	33.33	32.00	<ul style="list-style-type: none"> <li>corrosion near O-ring; slight slime; black spots on inside threads</li> <li>no moisture; "x" smeared</li> </ul>	1,4
01/03/02	33.62	21.38	<ul style="list-style-type: none"> <li>corrosion near O-ring; slight slime; black spots on inside threads</li> <li>no moisture; "x" smeared</li> </ul>	1,4
01/10/02	33.11	21.89	<ul style="list-style-type: none"> <li>corrosion near O-ring and on Gore-Tex; black spots on inside threads</li> <li>no moisture; "x" smeared</li> </ul>	1,4
01/17/02	32.69	5.00	<ul style="list-style-type: none"> <li>corrosion near O-ring and on Gore-Tex; black spots on inside threads</li> <li>moisture inside; droplets</li> </ul>	1,4
01/24/02	32.59	5.00	<ul style="list-style-type: none"> <li>corrosion near O-ring and on Gore-Tex; black spots on inside threads</li> <li>moisture inside; droplets</li> </ul>	1,4

<sup>1</sup> Water level taken with QED Yellow Jacket Interface Probe

<sup>2</sup> Water level taken with KECK Interface Probe

<sup>3</sup> Site 18 dual-extraction system operational during weekly inspection

<sup>4</sup> Site 18 dual-extraction system not operational during weekly inspection

## 2.2.2 Corrosion

Visual observations of the 304 stainless-steel housing during the test revealed that there were signs of possible corrosion and microbial degradation (see Table 1). Small black spots were observed on the inside threads of the housing after the 3<sup>rd</sup> week, and these continued to accumulate throughout the test. Crevice corrosion of the stainless-steel may have occurred on the threads, and the black spots were suspected to be magnetite (iron oxide), a product of oxidation. Observation under a magnifying glass showed that samples of the black material were planar, and the samples were attracted to a magnet when the samples were suspended in water. These observations support the speculation that the black spots were magnetite (a likely product of crevice corrosion).

A thin film of slime was also noted on the exterior of the housing by the 2<sup>nd</sup> week, and it continued to accumulate in subsequent weeks. The slime was likely an indication of microbial activity, but no further tests were performed to identify the cause of the slime. By the 5<sup>th</sup> week, slight corrosion of the steel near the O-ring was observed, and by the 9<sup>th</sup> week, a discoloration of the membrane was observed. Figure 8 shows images of the housing that provide evidence of corrosion and microbial activity during this test. It should be noted, however, that aside from the deliberate breach of the membrane, the overall integrity of the housing was maintained during the duration of this test. This was verified during tests in Phase III in which the chemiresistor sensor operated continuously underwater without fail at well 18-MW37 for a period of four months. The primary difference was that the sensor was maintained at a depth within five feet of the water table during the entire duration of Phase III (the water-entry pressure of the membrane was not exceeded).

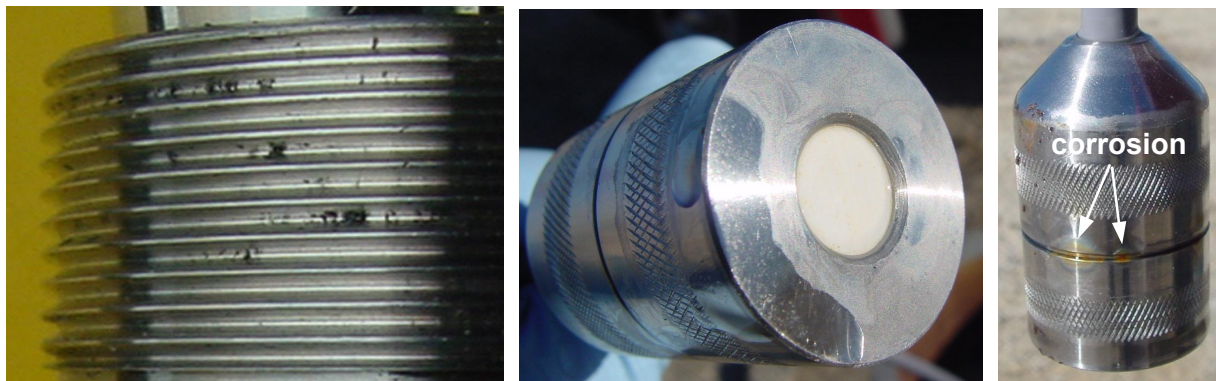


Figure 8. Evidence of corrosion and microbial activity. Left: Black spots were observed on the threads of the housing after 2 weeks of immersion. Middle: “Slime” observed at 9 weeks (began at 2 weeks). Right: Corrosion was observed near the seam and O-ring of the housing at 10 weeks (began at 5 weeks).

### 3. Phases II and III: Field Evaluation of Chemiresistor Performance in the Unsaturated and Saturated Zones

#### 3.1 Approach

Following the test of the chemiresistor housing in Phase I, the chemiresistor sensor itself was evaluated both in the unsaturated zone (Phase II) and saturated zone (Phase III) of well 18-MW37. A chemiresistor sensor (chip C12) was placed in the housing. The chip consisted of four different polymers (from left to right in Figure 2): polyepichlorohydrin (PECH), poly(N-vinyl pyrrolidone) (PNVP), polyisobutylene (PIB), and poly(ethylene-vinyl acetate) copolymer (PEVA). Each of these polymers was calibrated to TCE under different temperature and relative-humidity conditions in the laboratory prior to deployment in the field. Ideally, the combined response of these chemiresistors would be used in multivariate regression analyses (factor analysis) to account for the presence of water vapor and other analytes, but in this study the response of each polymer was investigated independently and without consideration to deviations in temperature and water-vapor concentrations. The purpose was to collect the “raw” unprocessed data to evaluate the impact of these variables on the response of the individual sensors. In addition, as detailed in Section 3.3, the TCE concentrations at the site were below the detection limits of the chemiresistor, so conducting a rigorous multivariate analysis would not be meaningful.

The chemiresistor probe was connected to a Campbell Scientific CR10X data logger via 65-ft long cable (Alpha 1299/20C 22 AWG). In addition, an Omega HX94C temperature/humidity probe and an Omega PX215 pressure transducer were connected via 100-ft cables to the data logger to record the temperature, relative humidity, and barometric pressure in the vicinity of the sensor (see Figure 9). A resistance temperature detector (RTD) on-board the chemiresistor chip was also used to record the local temperature of the chemiresistor sensor. The data logger was placed in a weatherproof enclosure that was mounted onto a steel tripod, which was anchored to

the ground (Figure 10). A 5-ft grounding rod was hammered into the ground and connected to a lightning rod mounted on top of the tripod. A 20-Watt solar panel mounted to the tripod was used to charge a 12 amp-hour battery connected to the data logger in the enclosure.



Figure 9. Left: Three sensors were deployed in Phases II and III (temperature/humidity probe, chemiresistor probe, and pressure transducer). Right: Tethering the sensors together before lowering them down well 18-MW37.



Figure 10. Left: Assembling the data-logging station at well 18-MW37. Right: Anchoring the tripod to the ground.

The sensors were lowered down well 18-MW37 to prescribed depths. For the Phase I test, the desired location of the chemiresistor sensor was just above the water table. For Phase II, the desired location was just below the water table. Table 2 summarizes the placement of the chemiresistor sensor relative to the water table at different times during the tests. It should be noted that because of the unpredictable fluctuation of the water table caused by the operation (and non-operation) of the nearby dual extraction system, the chemiresistor probe was

inadvertently submerged after a few days of the Phase I test. Figure 11 shows photos of the sensors being lowered down the well and the subsequent downloading of data. The data logger was programmed to collect and store data once every hour during the Phase II and Phase III tests (see Appendix for program). Although we manually downloaded the data using a laptop in these tests, wireless communication devices (e.g., a cell phone) can be easily integrated with the data logger so that data collection can be performed remotely and automatically.



Figure 11. Left: Lowering sensors down well 18-MW37. Middle: View of cables from top of well casing. Right: Downloading data from the data logger.

Table 2. Notable events during Phases II and III of chemiresistor operational tests.

Date	Event
5/28/02	Connected sensors (Omega HX94C temperature/humidity probe, Omega PX215 pressure transducer, and C12 chemiresistor sensor array) to Campbell CR10X data logger in Earth Tech trailer (23°C, ~24% RH, 13.5 psia).
5/29/02	Assembled data-logging station at well 18-MW37 and lowered sensors down well to 34 ft below top of casing (TOC), which was approximately 1 foot above the water table (at 35 ft below TOC). Began logging data every hour at 12:00 PM.
6/6/02	Downloaded data. Pulled the instruments out of the well and noticed a water stain on the cable of the chemiresistor probe, indicating that the water had immersed the chemiresistor probe by about a foot (the nearby dual-extraction system had shut down, which caused the water table to rise). Other instruments were tethered above the chemiresistor and were not submerged. Interior of chemiresistor housing was inspected and no moisture was seen inside. Chemiresistor probe was lowered to 32 ft below TOC, which was about a foot above the current water table (~33 ft below TOC). Begin Phase II.
6/25/02	Downloaded data. Water level measured at 33.9 ft below TOC. Chemiresistor probe now about 2 ft above water table.
6/27/02	Downloaded data. Pulled sensors from well. Replaced Gore-Tex membrane, which was half coated with golden-brown spots. Placed chemiresistor probe in clean Arrowhead water to re-baseline (T~23°C). Measured water level at 34.0 ft below TOC. Collected air sample in summa canister from 34 ft below TOC.

Date	Event
	Collected water samples in three 40 ml vials from 34.0-34.5 ft below TOC. Submitted samples for laboratory analysis. Placed chemiresistor probe 37 ft below TOC (3 ft below water table). Begin Phase III.
8/7/02	Downloaded data.
9/5/02	Downloaded data. Pulled instruments and immersed chemiresistor probe in distilled water for ~30 minutes to re-baseline. Measured water level at 35.6 ft below TOC. Performed transient test by lowering the chemiresistor probe 1 ft every 2 minutes starting at 37 ft below TOC to 54 ft below TOC (data were logged every 10 seconds). Raised chemiresistor probe ~ 1 ft/s and inspected interior; no moisture found inside. Lowered probe to 40 ft below TOC (4.4 ft below water table) and changed logging interval to once every hour.
9/19/02	Downloaded data. Measured water level at 35.6 ft below TOC.
10/9/02	Instruments pulled from well.

### 3.2 *Temperature, Pressure, and Relative Humidity*

The measured temperature in well 18-MW37 (between 32 and 40 ft below TOC) was quite constant during the duration of the Phase II and III tests. The average temperature recorded by the chemiresistor RTD while located in the well between May 29, 2002, and September 5, 2002, was 20.6 °C with a standard deviation of 0.32 °C. The Omega HX94C temperature/humidity probe also measured a similar temperature for several weeks, but at 3:00 PM, June 25, 2002, an anomaly occurred in the power supply (the battery voltage recorded a negative value), and the HX94C temperature/humidity probe malfunctioned. The other instruments recovered, but the HX94C probe did not work from that point on. Before the probe malfunctioned, the relative humidity was continuously recorded at 100%, both just above the water table and just below the water table. These stable values for temperature and relative humidity are conducive to the operation of the chemiresistor sensor. However, the large water-vapor concentrations at 100% relative humidity can cause condensation on the sensors.

The Omega PX215 pressure transducer recorded the barometric pressure in the well during the tests. Aside from an anomalously low reading at 3:00 PM, June 25, 2002, the pressure fluctuated between 925 and 940 mbars (converted from psia). Regressions between the pressure and the chemiresistor responses showed that these minor fluctuations in pressure did not impact the chemiresistor responses.

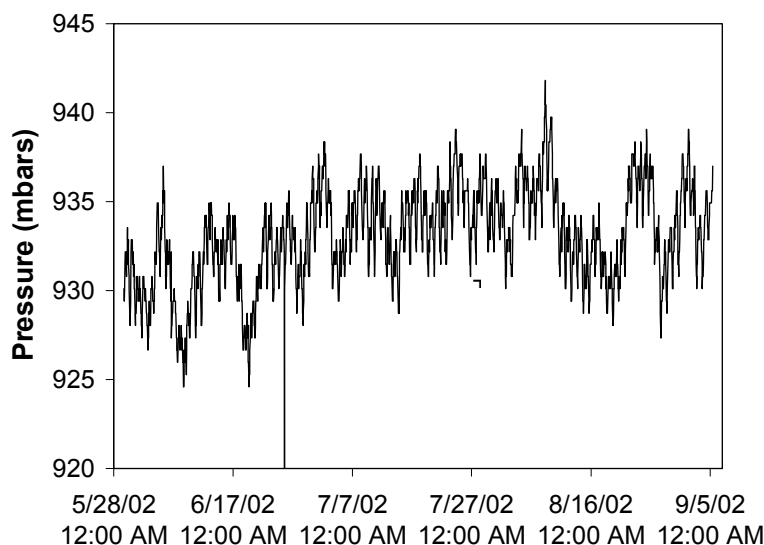


Figure 12. Barometric pressure in well 18-MW37.

### 3.3 Analytical Results from Laboratory Samples

As noted in Table 2, gas and liquid samples were taken from well 18-MW37 for VOC analysis on June 27, 2002. A Summa canister with 37 ft of Teflon tubing was used to pull a gas sample from just above the water table, and a Teflon bailer was used to collect liquid samples near the surface of the water table. The liquid samples were decanted into three 40 ml VOA vials for laboratory analysis. Table 3 presents the laboratory results for several of the primary VOC contaminants.

Table 3. Laboratory analysis of gas and liquid samples taken from 18-MW37.<sup>1</sup>

Compound	Vapor Concentration <sup>2</sup> (ppbv)	Aqueous Concentration <sup>3</sup> (µg/L or ppb)
Trichloroethylene (TCE)	5600	540
cis-1,2-dichloroethene	2100	340
1,2-dichloroethane	230	35

<sup>1</sup> Samples taken near the water table (34 ft below TOC) on June 27, 2002.

<sup>2</sup> Using Method TO14.

<sup>3</sup> Using EPA method SW8260.

The concentrations are significantly lower than those reported earlier. For example, aqueous TCE concentrations were measured at 10,000 µg/L on October 24, 2001. A likely reason for the difference is that the previous samples were taken near the screened interval of the well (between 85-100 ft) where contaminated water could flow. The current samples were taken near the surface of the water table, which was probably stagnant. The VOCs in this region could volatilize and diffuse upward through the well, diluting the concentrations.

An interesting note is that the reported vapor concentration of TCE (5600 ppbv) is lower than the equilibrium vapor concentration corresponding to the measured aqueous concentration of 540 µg/L. Using Henry's constant for TCE at 20°C (0.0071 m<sup>3</sup>-atm/mol; Gossett, 1987) and the molecular weight of TCE (131.39 g/mol), the equilibrium TCE vapor pressure for an aqueous concentration of 540 µg/L is calculated as  $2.9 \times 10^{-5}$  atm or 2.96 Pa. The local barometric pressure at the time the sample was collected was logged at 932 mbars or 93,200 Pa. The resulting equilibrium TCE vapor concentration is then equal to  $2.96/93,200 \times 1 \times 10^9 = 31,800$  ppbv. This calculated equilibrium vapor concentration is nearly six times greater than the measured vapor concentration. A possible reason for the discrepancy is that dilution may have occurred during sampling of the gas above the water table. Recall that a 37-ft long Teflon tube was used to draw gas into the Summa canister, and the dead volume inside the tube may have diluted the sample. In addition, the headspace above the water table may have been saturated with TCE vapors right at the liquid surface, but the TCE vapor concentration was probably diluted with increasing distance above the water table due to diffusion to the top of the well.

Unfortunately, the measured vapor concentrations were below the detection limits of the chemiresistor (without preconcentration). Even the estimated equilibrium TCE vapor concentration, which is much larger than the measured TCE vapor concentrations, is at the lower limits of detectability. As a result, there should be no responses from the chemiresistors in either the unsaturated or saturated zones when the chemiresistor was placed near the surface of the water table.

### **3.4 Chemiresistor Results**

#### **3.4.1 Initial Week-Long Test**

During the first week of testing, May 29, 2002 to June 6, 2002, the chemiresistor-sensor package was lowered approximately 34 ft below TOC at 18-MW37. The water table in the well at the beginning of the experiment was about 1 ft below the location of the sensor package. However, an unexpected rise in the water table, caused by the temporary shut-down of the nearby dual extraction remediation system, immersed the chemiresistor-sensor package. The original intent was to use a baseline resistance for each of the four polymers as measured in the Earth Tech trailer. The subsequent relative changes in resistances would then be used to calculate the TCE concentrations using the calibration curves developed in the laboratory.

However, as shown in Figure 13, some problems were evident. First, the chemiresistors showed a large response when placed in the well relative to the baseline resistance measured in the relatively dry environment in the trailer. While we expected a response to the 100% relative-humidity environment, the relative change was far greater than anything we observed in the lab. In addition, the resistances continued to increase during the week, with a noticeable jump between May 31 and June 1. This may have been an indication as to when the chemiresistor was immersed by the rising water table. We suspect that the large water-vapor concentration (and perhaps some film condensation) was causing water to continually absorb into the polymers, creating a "creeping" effect. Most of the polymers, however, did stabilize towards the end of the first week.

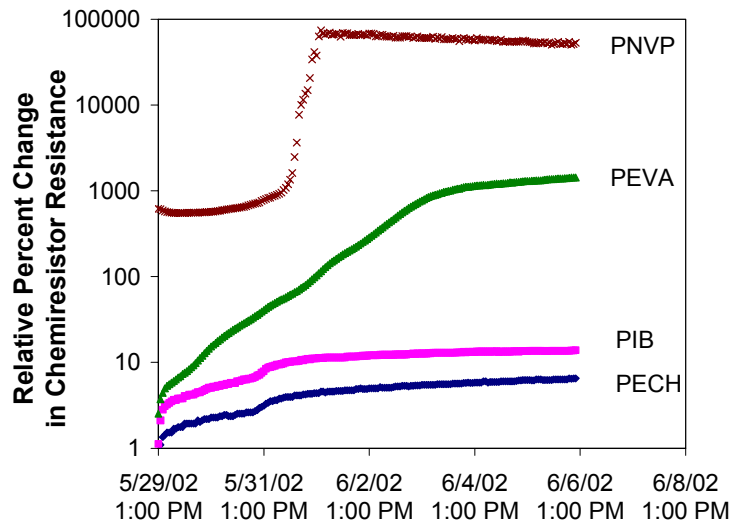


Figure 13. Response of the chemiresistor sensors during the first week. The chemiresistor probe was immersed by the rising water table. Baseline resistance was taken from dry conditions in the Earth Tech trailer (23°C, ~24% RH).

### 3.4.2 Unsaturated-Zone Test

Towards the end of the first week of testing, most of the chemiresistors showed signs of stabilization (see Figure 13). On June 6, the chemiresistor was pulled above the water table and suspended about a foot above the water table. The water table appeared to remain below the chemiresistor for the next several weeks, so the period between June 6 and June 25 was used for the Phase I (unsaturated-zone) test.

Figure 14 shows the relative change of the chemiresistor resistances during Phase II using resistances measured on June 6 as the baseline. These relative changes were used with the calibration curves to estimate the vapor concentration of TCE (Figure 15). Recall that the laboratory analyses indicated that the measured vapor concentrations were less than the detection limits of the chemiresistor. Therefore, we expect to see little, if any, estimated concentrations from the chemiresistor in the vapor phase. Deviations and drift from a zero value shown in Figure 15 are probably anomalous, caused by the large water-vapor concentrations present near the sensor. We suspect that creep caused by continual absorption of the water vapor on the polymer films caused the deviations.

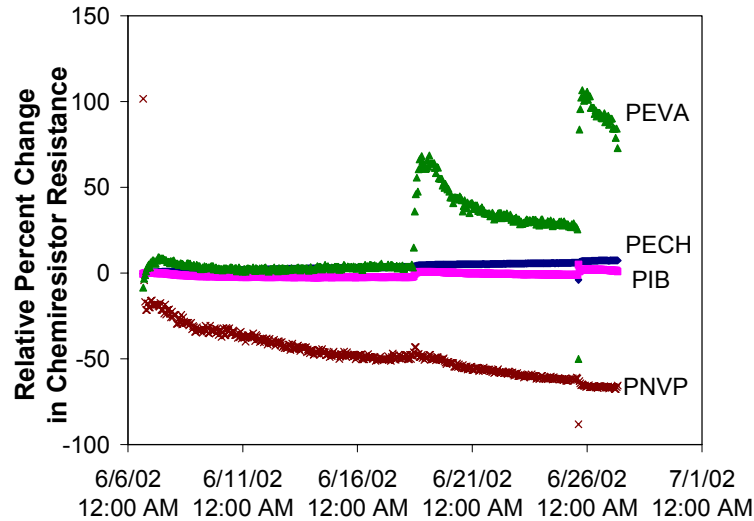


Figure 14. Relative percent change of the chemiresistor resistances during the Phase II unsaturated-zone test (June 6 – June 25, 2002). The baseline resistances were taken at the beginning of the test on June 6, 2002.

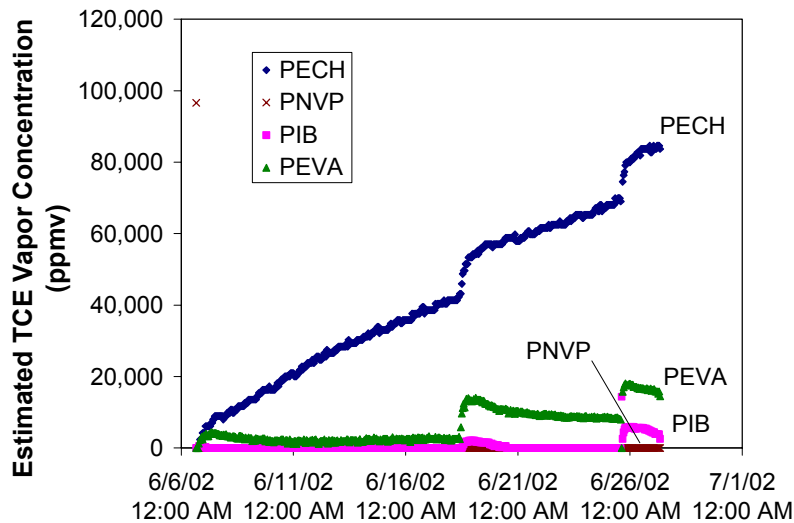


Figure 15. Estimated TCE vapor concentrations during the Phase II unsaturated-zone test.

### 3.4.3 Saturated-Zone Test

On June 27, 2002, Phase III commenced when the chemiresistor sensor was lowered about 2 ft below the water table. The chemiresistor was submerged continually for over two months until September 5, 2002, at which time the sensor was pulled from the well for a transient test (see Section 3.4.4 for details). Figure 16 shows the relative percent change in the response of the

chemiresistor resistances during the Phase III test. Again, recall that the laboratory analyses revealed that measured aqueous concentrations were lower than the detection limits of the chemiresistor sensor. Deviations from a zero value are likely caused by interferences from the large water vapor concentrations (as opposed to responses to VOCs).

Figure 17 shows the estimated aqueous concentrations using the responses from the chemiresistor sensor along with the calibration curves. Henry's Law was used to convert the vapor concentrations (estimated from the calibration curves) to aqueous concentrations. The large fluctuations appear to be anomalous based on the laboratory analysis. Sections 4 and 5 provide recommendations to correct these anomalies and provide improved stability for the chemiresistor sensor in high-humidity environments.

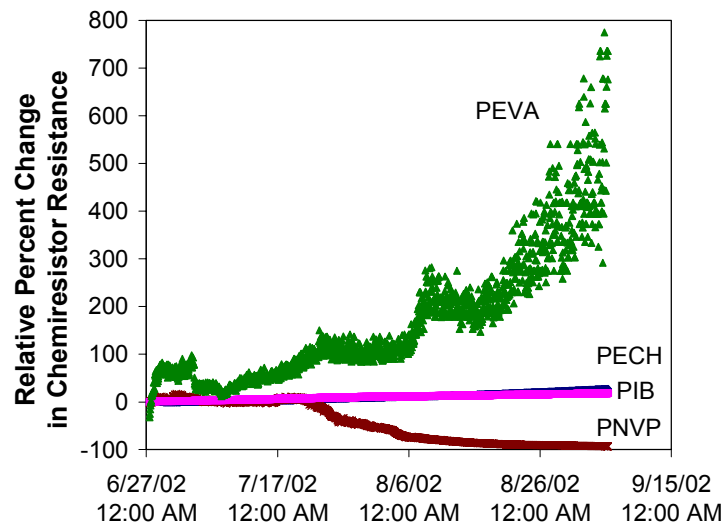


Figure 16. Relative percent change of the chemiresistor resistances during the Phase III unsaturated-zone test (June 27 – September 5, 2002). The baseline resistances were taken at the beginning of the test on June 27, 2002.

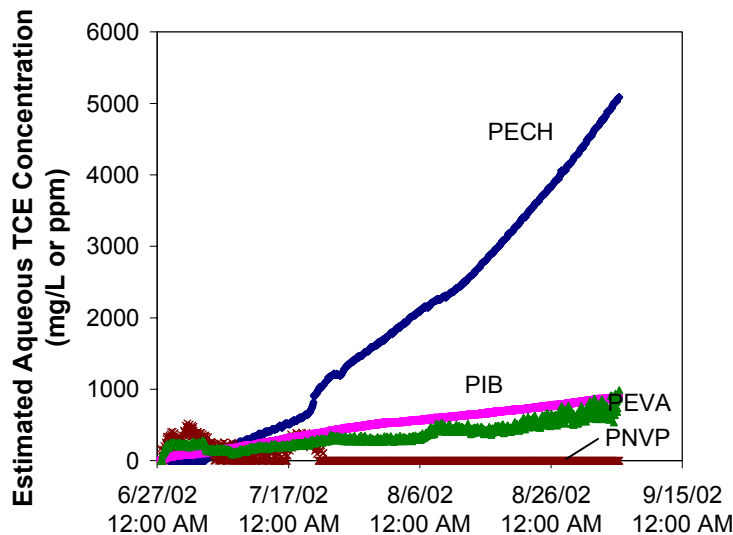


Figure 17. Estimated aqueous TCE concentrations during the Phase III saturated-zone test.

### 3.4.4 Transient Test

Because the laboratory samples taken from the surface of the water table at well 18-MW37 yielded concentrations that were too low for detection by the chemiresistor, a test was proposed to lower the chemiresistor into greater depths where the TCE concentration was higher. On September 5, 2002, the chemiresistor sensor was lowered gradually from a depth of 37 ft below TOC (water level was at a depth of 35.6 ft below TOC) to a depth of 54 ft below TOC. The chemiresistor probe was lowered 1 ft every two minutes, and data logging occurred once every 10 seconds. The sensor was then pulled to the surface. The objective was to see if an increase in chemiresistor response would be recorded upon lowering the sensor into regions with higher TCE concentrations. The chemiresistor response should then decrease upon raising the sensor.

Figure 18 shows the relative percent change in chemiresistor resistances resulting from this transient test. Unfortunately, no systematic trends in readings were observed. The resistance did increase, but the trend seemed to be due to the re-exposure of the chemiresistor to the 100% relative-humidity environment after it had been pulled from the well. We suspect that the sensor did not have enough time to equilibrate with the water before the test began (the chemiresistor was pulled from the well before the test to be cleaned and re-baselined). In addition, because of time constraints, the sensor was raised from the well too rapidly to determine if a systematic decrease in chemiresistor resistances could be observed.

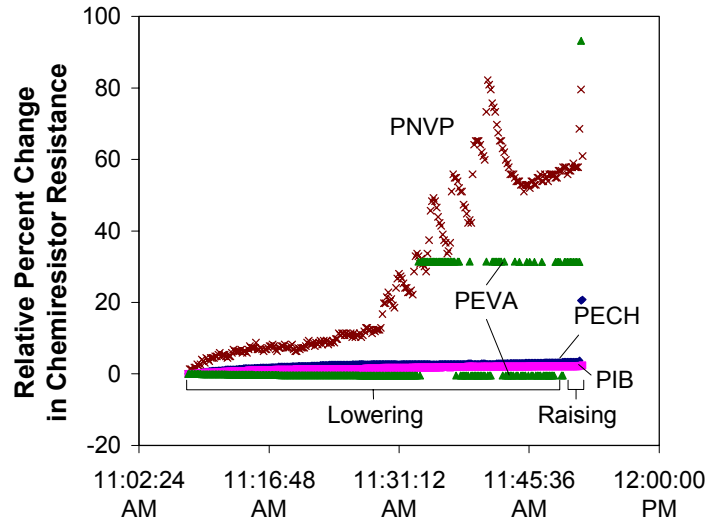


Figure 18. Relative percent change of the chemiresistor resistances during the transient test on September 5, 2002. The baseline resistances were taken while the chemiresistor was suspended 37 ft below TOC.

### 3.4.5 Results of Long-Term Evaluation

One of the general objectives of the field tests was to determine the long-term operation capabilities of the chemiresistor sensor. Figure 19 shows the measured resistances from the four polymers used in the chemiresistor sensor during the entire time it was placed in well 18-MW37. Although the results were often spurious, one positive observation was that the chemiresistor sensor provided continuous output during its operation over a four-month period in corrosive aqueous environments. The sharp changes in resistances that were recorded in Figure 19 are often correlated to events where the sensor was taken out of the well, handled, and placed back in the well for the start of a new phase or test.

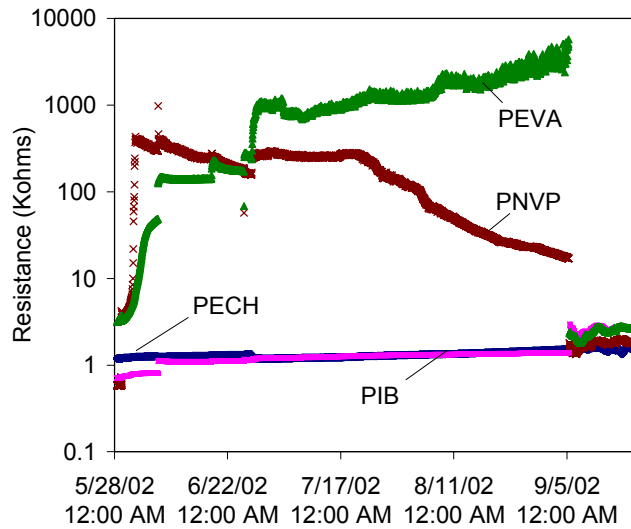


Figure 19. Measured chemiresistor resistances during all field tests (May – September 2002).

## 4. Discussion of Results and Objectives

The results of the field tests at Edwards AFB have provided useful insights regarding the design, operation, and performance of the chemiresistor sensors in actual field environments. The specific results of the tests as related to the detailed objectives of the Edwards AFB In-Situ Sensor Program are detailed below.

### 4.1 Objectives of Edwards Air Force Base In-Situ Sensor Program

The detailed objectives of the In-situ Sensor Program developed by Edwards AFB are as follows:

1. To evaluate the longevity of the housing of the sensor
2. To compare concentrations measured from sensor vs. fixed lab results
3. To evaluate the detection limits and ranges of the sensors
4. To evaluate use of the sensors for various measurements in vapor and water and for use as a screening tool vs. a more quantitative measurement
5. To evaluate the repeatability of measurements of the sensors
  - a. Evaluate repeatability of the sensor readouts (relative to lab results)
  - b. Evaluate sensor's ability to recalibrate itself
6. To evaluate the operation and maintenance requirements of the sensor
7. To answer how each sensor would fit into the operation and maintenance and/or long-term monitoring tasks at Edwards AFB

8. To evaluate if or how sensors could reduce operation and maintenance and/or LTM costs

The following subsections describe the results of the field tests in the context of these specific objectives.

#### **4.2 Objective 1: Longevity of Sensor Housing**

Although signs of corrosion on the housing were observed during the Phase I test, the integrity of the housing was maintained throughout the tests during FY02. The chemiresistor sensor operated continuously throughout Phases II and III while submerged underwater, and the Gore-Tex<sup>®</sup> membrane prevented liquid water from entering the housing as long as the water-entry-pressure threshold (~30 feet as determined from Phase I testing) was not exceeded. It appears that the design of the chemiresistor housing is robust and can last for at least a year, but housings made from plastic (e.g., PEEK) may be desirable for long-term applications to prevent corrosion. The Gore-Tex<sup>®</sup> membrane may need to be replaced once or twice a year if the housing is submerged in water. The Viton O-ring did not appear to exhibit any deterioration during the tests.

#### **4.3 Objectives 2, 3, 4, and 5: Chemiresistor Performance**

Results of the field tests indicate that the chemiresistor sensor was not stable in high-humidity environments (both in the unsaturated zone just above the water table and in the saturated zone). Comparison to lab results (objectives 2 and 3) showed that TCE concentrations estimated from the response of the chemiresistors were significantly greater than values obtained from laboratory analyses of gas and water samples from the same location.

The repeatability and stability of the chemiresistor (objective 5) was compromised, we believe, by the high-humidity environments. The 100% relative humidity environments were conducive to condensation that may have caused a continual sorption (creep) in the polymers. We propose that maintaining the local temperature of the sensor above the ambient may help to prevent condensation and stabilize the sensor. This can be accomplished by using heating elements and a temperature sensor already on-board the sensor chip (see Figure 2) combined with a simple automated temperature-control algorithm programmed in the data logger.

Another issue regarding the performance of the chemiresistors is the detection limit. The detection limit of the chemiresistor sensor (objective 3) was determined in the lab to be approximately 0.1% of the saturated vapor pressure for TCE and other volatile organic compounds. For TCE, this corresponds to approximately 100 ppmv in the vapor phase. The low concentrations of VOCs near the surface of the water table in monitoring well 18-MW37, compounded with the instability of the chemiresistor sensors, made it difficult to evaluate the detection capabilities of the chemiresistor sensor in these tests.

A preconcentrator assembly has recently been developed at Sandia National Laboratories to increase the sensitivity of the chemiresistor by potentially several orders of magnitude. The preconcentrator consists of a “micro-hotplate” that is coated with a sorbent to collect VOCs.

After a period of time during which the preconcentrator is loaded with VOCs, a voltage is applied across the micro-hotplate to heat the sorbent rapidly to high temperatures and desorb the VOCs. The high-concentration plume of VOCs is then sensed by the nearby chemiresistor. The preconcentrator assembly has been recently integrated with the chemiresistor package (Figure 20). Preliminary laboratory tests show that the integrated preconcentrator is functioning well and can increase the detection limit for TCE by up to two orders of magnitude.

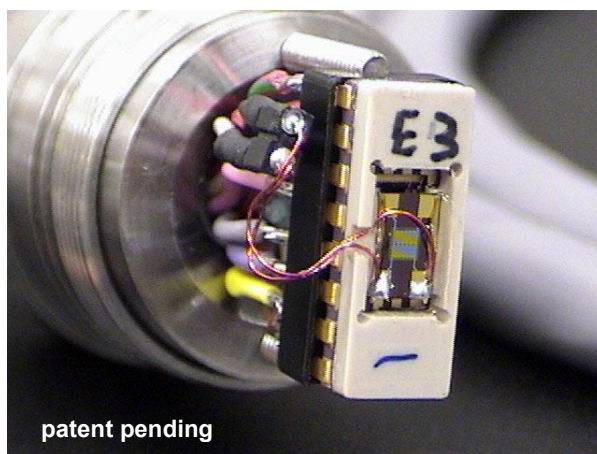


Figure 20. Integrated preconcentrator/chemiresistor assembly in the waterproof package.

#### **4.4 Objective 6: Operation and Maintenance Requirements**

The operation and maintenance requirements (objective 6) of the chemiresistor sensor were minimal. The solar-powered data-logging stations operated continuously over a four-month period. The only manual intervention was to periodically download the data, but the simple addition of a cell phone and modem would eliminate the need to manually download the data. The sensor operated continuously during the four-month test, but the results were not stable. Additional maintenance requirements may be needed to re-calibrate the sensors periodically, depending on how well the automated temperature control improves the stability. In-situ calibration methods that utilize a purge gas carried from the surface to the sensor via tube are being investigated.

#### **4.5 Objectives 7 and 8: Potential Use at Edwards Air Force Base**

Current results show that the chemiresistor sensor is impacted by high-humidity environments. Until automated-temperature-control features can be tested, our current recommendations are to use the chemiresistor sensors as screening tools in the vadose zone or in applications with less than 100%-humidity environments. The implementation of a preconcentrator with the chemiresistor will likely increase the sensitivity and relax the need for long-term stability, but these integrated devices have not yet been tested in the field.

We believe that significant advancements in the chemiresistor technology (including automated temperature control and preconcentrators) can be made in a year with further testing in the laboratory and in the field. Nevertheless, we feel confident that the chemiresistor sensors can be used currently to monitor significant changes in VOC concentrations. The slow, long-term creep exhibited by the chemiresistors can be accounted for in the data-processing algorithm so that only significant changes in the response are noted.

## 5. Summary and Recommendations

Field tests of the chemiresistor sensor were performed at Edwards Air Force Base to evaluate the ruggedness of the chemiresistor sensor package and the performance of the sensor in an actual field environment. In the first phase of testing, the housing was submerged beneath the water table at well 18-MW37. The housing was lowered deeper and deeper beneath the water table until leaking was observed. In the second and third phases of testing, a chemiresistor sensor was placed in the housing and connected via cable to a data logging station that operated continuously using solar power. The sensor was lowered down the well and operated for a period of time in both the unsaturated and saturated zones. Major findings and recommendations regarding these tests are detailed below.

- The 304 stainless-steel housing showed signs of corrosion over the course of the tests. The operation of the chemiresistor sensor was not adversely impacted, but the use of plastic housings (e.g., PEEK) may decrease the corrosion of the housing in oxidizing aqueous environments.
- The Gore-Tex<sup>®</sup> polymer membrane prevented liquid water from entering the housing up to depths of ~30 ft.
- The chemiresistor sensor operated continuously over a four-month period in well 18-MW37 using a Campbell Scientific data logger powered by a 12 amp-hour battery and 20-Watt solar panel. Data were logged from the station manually using a laptop and serial connection; we recommend implementing a cell phone modem (or other wireless communications device) for the capability to log data remotely and automatically.
- The measured concentrations (using off-site laboratory analysis of grab samples) near the surface of the water table at well 18-MW37 were too low for detection by the chemiresistor, so direct comparisons could not be made. The use of an integrated preconcentrator assembly to increase the detection limits of the chemiresistor is currently being investigated. Additional tests in wells with higher concentrations (> 1000 ppmv) is desired.
- The results of all four polymers on the chemiresistor sensor chip showed instability during the field tests, even though the temperature and relative humidity were nearly constant (~21°C, 100% RH). Estimated concentrations using the chemiresistor readings were anomalously high. We speculate that the large water-vapor concentrations (100% relative-humidity environments) may

have caused condensation and spurious readings (continual sorption and creep of the polymers). The use of automated temperature control to keep the chip temperature above the local ambient may prevent condensation and improve the stability.

- Potential use of the chemiresistor sensor (in its current state) at Edwards AFB appears to be limited to screening analyses in applications with large changes (> thousands of ppmv) in VOC concentrations. This assessment is based on evaluations of the chemiresistor in controlled laboratory environments. These sensors can also potentially be used for “confidence monitoring” (as opposed to compliance monitoring) at sites where continuous monitoring for long-term changes in VOC concentrations is required. Improvements to the chemiresistor (e.g., preconcentrator for improved sensitivity and temperature control for better stability and repeatability) are likely to expand the potential role of the chemiresistor sensor for field applications.

## 6. References

Gossett, J.M., 1987, Measurement of Henry’s Law Constants for C<sub>1</sub> and C<sub>2</sub> Chlorinated Hydrocarbons, *Environ. Sci. Technol.*, 21, 202-208.

Ho, C.K., and R.C. Hughes, 2002, *In-Situ* Chemiresistor Sensor Package for Real-Time Detection of Volatile Organic Compounds in Soil and Groundwater, 2002, *Sensors*, 2, 23-34.

Hughes, R.C.; Casalnuovo, S.A.; Wessendorf, K.O.; Savignon, D.J.; Hietala, S; Patel, S.V.; and Heller, E.J., 2000, Integrated Chemiresistor Array for Small Sensor Platforms, *SPIE Proceedings Paper 4038-62*, p. 519, AeroSense 2000, April 24-28, 2000, Orlando, Florida.

## 7. Appendices

### 7.1 Appendix A: Campbell Scientific CR10X Data-Logging Program

```
;{CR10X}
;
*Table 1 Program
  01: 3600      Execution Interval (seconds)

1: Batt Voltage (P10)
  1: 1          Loc [ Vbatt      ]

2: Do (P86)
  1: 1          Call Subroutine 1

3: Excite-Delay (SE) (P4);This reads PECH
  1: 1          Reps
  2: 5          2500 mV Slow Range
  3: 6          SE Channel
  4: 1          Excite all reps w/Exchan 1
  5: 10         Delay (units 0.01 sec)
  6: 2500       mV Excitation
  7: 2          Loc [ Sen_1_mVm ]
  8: -1         Mult
  9: 0          Offset

4: Excite-Delay (SE) (P4);This reads PNVP
  1: 1          Reps
  2: 5          2500 mV Slow Range
  3: 2          SE Channel
  4: 1          Excite all reps w/Exchan 1
  5: 10         Delay (units 0.01 sec)
  6: 2500       mV Excitation
  7: 3          Loc [ Sen_2_mVm ]
  8: -1         Mult
  9: 0          Offset

5: Excite-Delay (SE) (P4);This reads PIB
  1: 1          Reps
  2: 5          2500 mV Slow Range
  3: 3          SE Channel
  4: 1          Excite all reps w/Exchan 1
  5: 50         Delay (units 0.01 sec)
  6: 2500       mV Excitation
  7: 4          Loc [ Sen_3_mVm ]
  8: -1         Mult
  9: 0          Offset

6: Excite-Delay (SE) (P4);This reads PEVA
  1: 1          Reps
  2: 5          2500 mV Slow Range
  3: 4          SE Channel
  4: 1          Excite all reps w/Exchan 1
  5: 10         Delay (units 0.01 sec)
  6: 2500       mV Excitation
  7: 5          Loc [ Sen_4_mVm ]
  8: -1         Mult
  9: 0          Offset

7: Excite-Delay (SE) (P4);This reads the
RTD
  1: 1          Reps
  2: 5          2500 mV Slow Range
  3: 5          SE Channel

  4: 2          Excite all reps w/Exchan 2
  5: 10         Delay (units 0.01 sec)
  6: 2500       mV Excitation
  7: 6          Loc [ Sen_5_mVm ]
  8: -1         Mult
  9: 0          Offset

8: Volt (SE) (P1) This reads HX94 temp
  1: 1          Reps ;
  2: 05         2500 mV Slow Range ;
  3: 8          SE Channel
  4: 36         Loc [ TempNum   ]
  5: .001       Mult
  6: 0.0        Offset

9: Volt (SE) (P1) This reads HX94 RH
  1: 1          Reps
  2: 05         2500 mV Slow Range
  3: 11         SE Channel
  4: 37         Loc [ RHNum     ]
  5: .001       Mult
  6: 0.0        Offset

10: Volt (SE) (P1) This reads PX215 PSI
  1: 1          Reps
  2: 05         2500 mV Slow Range
  3: 12         SE Channel
  4: 38         Loc [ PSINum    ]
  5: .001       Mult
  6: 0.0        Offset

11: Z=X+F (P34)
  1: 2          X Loc [ Sen_1_mVm ]
  2: 2500       F
  3: 7          Z Loc [ Res_1_mVc ]

12: Z=X+F (P34)
  1: 3          X Loc [ Sen_2_mVm ]
  2: 2500       F
  3: 12         Z Loc [ Res_2_mVc ]

13: Z=X+F (P34)
  1: 4          X Loc [ Sen_3_mVm ]
  2: 2500       F
  3: 15         Z Loc [ Res_3_mVc ]

14: Z=X+F (P34)
  1: 5          X Loc [ Sen_4_mVm ]
  2: 2500       F
  3: 8          Z Loc [ Res_4_mVc ]

15: Z=X+F (P34)
  1: 6          X Loc [ Sen_5_mVm ]
  2: 2500       F
  3: 9          Z Loc [ Res_5_mVc ]

16: Z=X/Y (P38)
  1: 7          X Loc [ Res_1_mVc ]
  2: 10         Y Loc [ Ref1_Kohm ]
  3: 11         Z Loc [ uA_1c   ]
```

```

17:  Z=X/Y (P38)
   1: 12      X Loc [ Res_2_mVc ]
   2: 13      Y Loc [ Ref2_Kohm ]
   3: 14      Z Loc [ uA_2c      ]

18:  Z=X/Y (P38)
   1: 15      X Loc [ Res_3_mVc ]
   2: 16      Y Loc [ Ref3_Kohm ]
   3: 17      Z Loc [ uA_3c      ]

19:  Z=X/Y (P38)
   1: 8       X Loc [ Res_4_mVc ]
   2: 18      Y Loc [ Ref4_Kohm ]
   3: 19      Z Loc [ uA_4c      ]

20:  Z=X/Y (P38)
   1: 9       X Loc [ Res_5_mVc ]
   2: 20      Y Loc [ Ref5_Kohm ]
   3: 21      Z Loc [ uA_5c      ]

21:  Z=X/Y (P38)
   1: 2       X Loc [ Sen_1_mVm ]
   2: 11      Y Loc [ uA_1c      ]
   3: 22      Z Loc [ negkohms1 ]

22:  Z=X/Y (P38)
   1: 3       X Loc [ Sen_2_mVm ]
   2: 14      Y Loc [ uA_2c      ]
   3: 23      Z Loc [ negkohms2 ]

23:  Z=X/Y (P38)
   1: 4       X Loc [ Sen_3_mVm ]
   2: 17      Y Loc [ uA_3c      ]
   3: 24      Z Loc [ negkohms3 ]

24:  Z=X/Y (P38)
   1: 5       X Loc [ Sen_4_mVm ]
   2: 19      Y Loc [ uA_4c      ]
   3: 25      Z Loc [ negkohms4 ]

25:  Z=X/Y (P38)
   1: 6       X Loc [ Sen_5_mVm ]
   2: 21      Y Loc [ uA_5c      ]
   3: 26      Z Loc [ negkohms5 ]

26:  Z=X*F (P37)
   1: 22      X Loc [ negkohms1 ]
   2: -1      F
   3: 54      Z Loc [ PECH      ]

27:  Z=X*F (P37)
   1: 23      X Loc [ negkohms2 ]
   2: -1      F
   3: 55      Z Loc [ PVNP      ]

28:  Z=X*F (P37)
   1: 24      X Loc [ negkohms3 ]
   2: -1      F
   3: 56      Z Loc [ PIB       ]

29:  Z=X*F (P37)
   1: 25      X Loc [ negkohms4 ]
   2: -1      F
   3: 57      Z Loc [ PEVA      ]

30:  Z=X*F (P37)
   1: 26      X Loc [ negkohms5 ]
   2: -1      F
   3: 58      Z Loc [ RTD       ]

31:  Z=X-Y (P35)
   1: 36      X Loc [ TempNum   ]
   2: 39      Y Loc [ TempNum1  ]
   3: 40      Z Loc [ TempNumer ]

32:  Z=X/Y (P38)
   1: 40      X Loc [ TempNumer ]
   2: 41      Y Loc [ TempDenom ]
   3: 42      Z Loc [ TempMult  ]

33:  Z=X*F (P37)
   1: 42      X Loc [ TempMult  ]
   2: 100     F
   3: 59      Z Loc [ ProbeTemp ]

34:  Z=X-Y (P35)
   1: 37      X Loc [ RHNum     ]
   2: 44      Y Loc [ RHNum1    ]
   3: 48      Z Loc [ RHNumer   ]

35:  Z=X/Y (P38)
   1: 48      X Loc [ RHNumer   ]
   2: 45      Y Loc [ RHDenom   ]
   3: 49      Z Loc [ RHmult    ]

36:  Z=X*F (P37)
   1: 49      X Loc [ RHmult    ]
   2: 100     F
   3: 60      Z Loc [ ProberH  ]

37:  Z=X-Y (P35)
   1: 38      X Loc [ PSINum    ]
   2: 46      Y Loc [ PSINum1   ]
   3: 51      Z Loc [ PSINumer  ]

38:  Z=X/Y (P38)
   1: 51      X Loc [ PSINumer  ]
   2: 47      Y Loc [ PSIDenom  ]
   3: 52      Z Loc [ PSImult   ]

39:  Z=X*F (P37)
   1: 52      X Loc [ PSImult   ]
   2: 30      F
   3: 61      Z Loc [ PSI       ]

40:  If time is (P92)
   1: 00      Minutes (Seconds --) into a
   2: 60      Interval (same units as above)
   3: 10      Set Output Flag High (Flag 0)

41:  Resolution (P78)
   1: 00      Low Resolution

42:  Real Time (P77)
   1: 0220    Day,Hour/Minute (midnight =
2400)

43:  Sample (P70)
   1: 5       Reps
   2: 54      Loc [ PECH      ]

44:  Sample (P70)
   1: 3       Reps
   2: 59      Loc [ ProbeTemp ]

45:  Sample (P70)
   1: 1       Reps
   2: 1       Loc [ Vbatt     ]

*Table 2 Program
   02: 00      Execution Interval (seconds)

```

\*Table 3 Subroutines

```

1: Beginning of Subroutine (P85)
  1: 1      Subroutine 1

2: Z=F (P30)
  1: 2.3649 F
  2: 0      Exponent of 10
  3: 10     Z Loc [ Ref1_Kohm ]

3: Z=F (P30)
  1: 1.3276 F
  2: 00     Exponent of 10
  3: 13     Z Loc [ Ref2_Kohm ]

4: Z=F (P30)
  1: 2.6639 F
  2: 00     Exponent of 10
  3: 16     Z Loc [ Ref3_Kohm ]

5: Z=F (P30)
  1: 2.1990 F
  2: 00     Exponent of 10
  3: 18     Z Loc [ Ref4_Kohm ]

6: Z=F (P30)
  1: 1.2080 F
  2: 00     Exponent of 10
  3: 20     Z Loc [ Ref5_Kohm ]

7: Z=F (P30)
  1: .486   F
  2: 00     Exponent of 10
  3: 39     Z Loc [ TempNum1 ]

8: Z=F (P30)
  1: 1.942  F
  2: 00     Exponent of 10
  3: 41     Z Loc [ TempDenom ]

9: Z=F (P30)
  1: .483   F
  2: 00     Exponent of 10
  3: 44     Z Loc [ RHNum1 ]

10: Z=F (P30)
  1: 1.933  F
  2: 00     Exponent of 10
  3: 45     Z Loc [ RHDenom ]

11: Z=F (P30)
  1: .484   F
  2: 00     Exponent of 10
  3: 46     Z Loc [ PSINum1 ]

12: Z=F (P30)
  1: 1.936  F
  2: 00     Exponent of 10
  3: 47     Z Loc [ PSIDenom ]

13: End (P95)

End Program

-Input Locations-
1 Vbatt      1 1 1
2 Sen_1_mVm 1 2 1
3 Sen_2_mVm 1 2 1
4 Sen_3_mVm 1 2 1
5 Sen_4_mVm 1 2 1

```

```

6 Sen_5_mVm 1 2 1
7 Res_1_mVc 1 1 1
8 Res_4_mVc 1 1 1
9 Res_5_mVc 1 1 1
10 Ref1_Kohm 1 1 1
11 uA_1c     1 1 1
12 Res_2_mVc 1 1 1
13 Ref2_Kohm 1 1 1
14 uA_2c     1 1 1
15 Res_3_mVc 1 1 1
16 Ref3_Kohm 1 1 1
17 uA_3c     1 1 1
18 Ref4_Kohm 1 1 1
19 uA_4c     1 1 1
20 Ref5_Kohm 1 1 1
21 uA_5c     1 1 1
22 negkohms1 1 1 1
23 negkohms2 1 1 1
24 negkohms3 1 1 1
25 negkohms4 1 1 1
26 negkohms5 1 1 1
27 kohms_1c  1 0 0
28 kohms_2c  1 0 0
29 kohms_3c  1 0 0
30 kohms_4c  1 0 0
31 kohms_5c  1 0 0
32 Ref_temp  1 0 0
33 Ttype     1 0 0
34 _____ 0 0 0
35 _____ 0 0 0
36 TempNum   1 1 1
37 RHNum     1 1 1
38 PSINum    1 1 1
39 TempNum1  1 1 1
40 TempNumer 1 1 1
41 TempDenom 1 1 1
42 TempMult  1 1 1
43 _____ 0 0 0
44 RHNum1    1 1 1
45 RHDenom   1 1 1
46 PSINum1   1 1 1
47 PSIDenom  1 1 1
48 RHNumer   1 1 1
49 RHmult    1 1 1
50 _____ 0 0 0
51 PSINumer  1 1 1
52 PSImult   1 1 1
53 _____ 0 0 0
54 PECH      1 1 1
55 PVNP      1 1 1
56 PIB       1 1 1
57 PEVA      1 1 1
58 RTD       1 1 1
59 ProbeTemp 1 1 1
60 ProbeRH   1 1 1
61 PSI       1 1 1
-Program Security-
0000
0000
0000
-Mode 4-
-Final Storage Area 2-
0
-CR10X ID-
0
-CR10X Power Up-
3

```

## 7.2 Appendix B: Calibration Curves for Chemiresistor Sensor

The calibration of the chemiresistor array was performed by introducing known concentrations of TCE and water vapor to each of the four polymers on chip C12 (from left to right in Figure 2): polyepichlorohydrin (PECH), poly(N-vinyl pyrrolidone (PNVP), polyisobutylene (PIB), and poly(ethylene-vinyl acetate) copolymer (PEVA). Digitally controlled mass-flow controllers were used to maintain precise flow rates of pure nitrogen through bubblers containing liquid TCE and water to the chemiresistor polymers. The tests were conducted at two different chemiresistor temperatures: 22 °C (room temperature (RT)) and 30 °C (in a controlled oven). In addition, the TCE exposures were conducted at two different relative humidities: 0% (pure TCE in nitrogen) and 100% relative humidity (RH) at room temperature. In the latter case, controlled amounts of TCE vapor were passed through the water bubbler until the water reached equilibrium with the flowing TCE vapor. This allowed known concentrations of TCE to be introduced to the chemiresistor polymers under 100% relative humidity conditions. Figure 21 through Figure 24 shows the results of these calibrations.

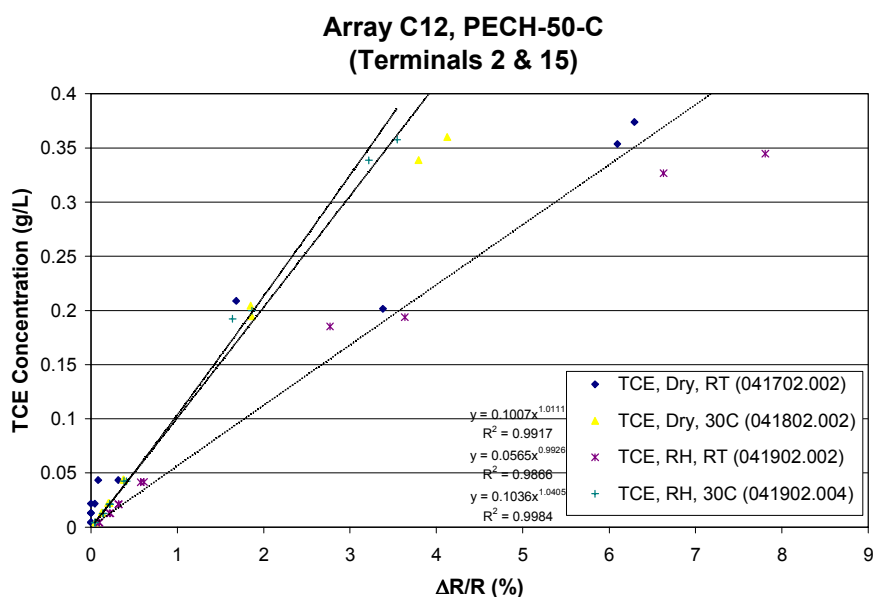


Figure 21. Calibration curves for PECH polymer on chip C12.

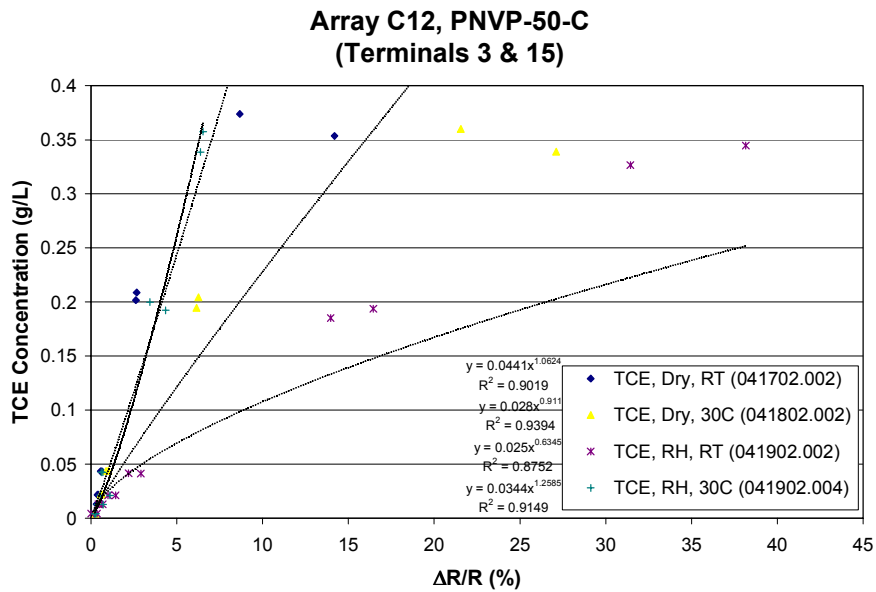


Figure 22. Calibration curves for PNVP polymer on chip C12.

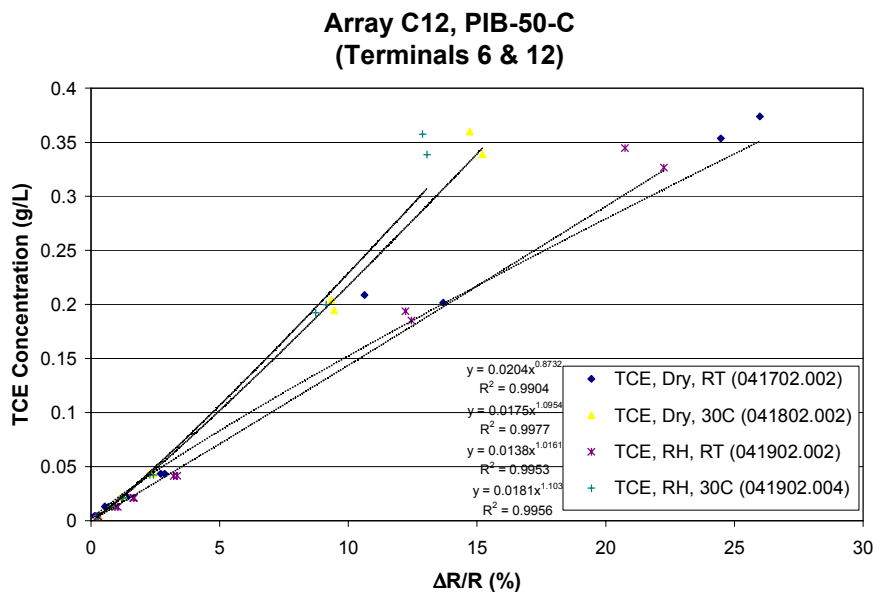


Figure 23. Calibration curves for PIB polymer on chip C12.

**Array C12, PEVA-40-C  
(Terminals 6 & 11)**

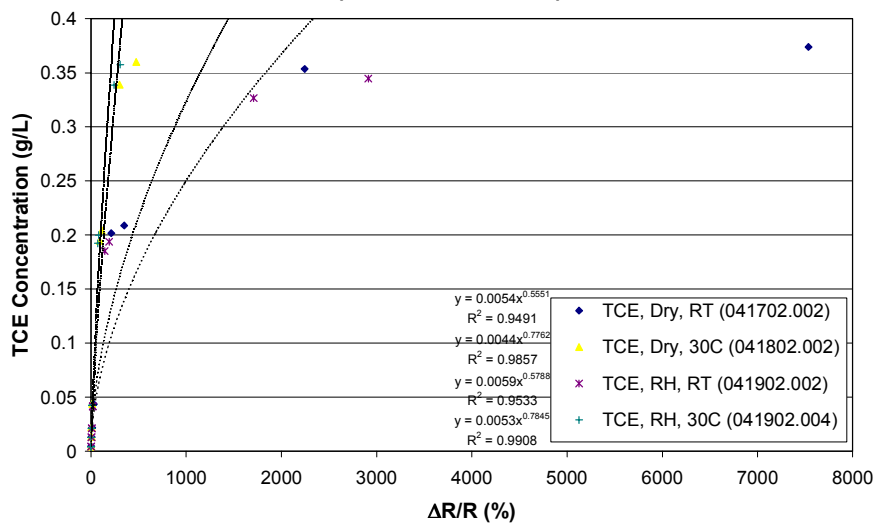


Figure 24. Calibration curves for PEVA polymer on chip C12.

## Distribution

### External

Mary Spencer  
AFFTC/EMR  
5 East Popson Avenue, Bldg. 2650A  
Edwards AFB, CA 93524-1130

James Specht  
AFFTC/EMRR  
5 E. Popson Ave, Bldg. 2650A  
Edwards AFB CA 93524-1130

Irene Nester  
Tybrin Corporation  
5 East Popson Avenue, Bldg. 2650A  
Edwards AFB, CA 93524-1130

James May  
Earth Tech  
100 West Broadway, Suite 240  
Long Beach, CA 90802-4443

Tara MacHarg  
Earth Tech  
100 West Broadway, Suite 5000  
Long Beach, CA 90802-4443

Randy Olsen  
U.S. Army Corps of Engineers  
1325 J Street  
Sacramento, CA 95814-2922

Susan Yarbrough  
U.S. Army Corps of Engineers  
1325 J Street  
Sacramento, CA 95814-2922

### Internal

1 MS-0113 S. Hagerman, 1322  
1 MS-1079 M. Scott, 1700  
1 MS-1425 S. Martin, 1707  
1 MS-1425 R. Hughes, 1744  
1 MS-1425 S. Casalnuovo, 1744  
1 MS-1425 C. Davis, 1744  
1 MS-1425 M. Thomas, 1744  
1 MS-0892 R. Cernosek, 1764  
1 MS-0865 R. Stinnett, 1903  
1 MS-0701 P. Davies, 6100  
1 MS-0701 W. Cieslak, 6100  
1 MS-0706 R. Finley, 6113  
10 MS-0735 C. Ho, 6115  
3 MS-0735 L. McGrath, 6115  
1 MS-0735 E. Webb, 6115  
1 MS-0750 M. Walck, 6116  
1 MS-0750 D. Borns, 6116  
1 MS-0751 L. Costin, 6117  
1 MS-0750 H. Westrich, 6118  
1 MS-0719 W. Cox, 6131  
1 MS-0719 S. Howarth, 6131  
1 MS-0719 E. Lindgren, 6131  
1 MS-1087 F. Nimick, 6132  
1 MS-1087 D. Stockham, 6133  
1 MS-1088 D. Miller, 6134  
1 MS-1089 D. Fate, 6135  
1 MS-0755 W. Einfeld, 6233  
1 MS-1395 Y. Wang, 6822

1 MS-9018 Central Technical Files, 8945-1  
2 MS-0899 Technical Library, 9616  
1 MS-0612 Review & Approval Desk, 9612  
For DOE/OSTI